Progress In Electromagnetics Research, Vol. 123, 13–30, 2012

GENERALIZED EQUIVALENT CABLE BUNDLE METHOD FOR MODELING EMC ISSUES OF COMPLEX CABLE BUNDLE TERMINATED IN ARBITRARY LOADS

Z. Li[1, 2, *], L. L. Liu[1], and C. Q. Gu[1]

[1]College of Electronic and Information Engineering, Nanjing University of Aeronautics and Astronautics, Nanjing 210016, China

[2]State Key Laboratory of Millimeter Waves, Southeast University, Nanjing 210096, China

Abstract—A generalized equivalent cable bundle method (GECBM) is presented for modeling electromagnetic (EM) compatibility issues of complex cable bundle terminated in arbitrary loads. By introducing a new grouping criterion, complex cable bundles terminated in arbitrary loads can be reasonably simplified through a generalized equivalence procedure. The reduced cable bundle model can be used for modeling electromagnetic immunity, emission and crosstalk problems. The complexity and the computation time for the complete cable bundle modeling has been significantly reduced and fairly good precision is maintained. Numerical simulations are given to validate the efficiency and advantages of the method.

1. INTRODUCTION

Cable and cable bundle networks are commonly used in connecting all the electronic equipment interfaces in various vehicles, from a car to an airplane. To make the vehicles more comfortable and spacious, much of the installation space for the cables and cable bundles is reduced. Thus, the densely packed cables and cable bundles expose a lot of electromagnetic compatibility (EMC) problems, immunity from external high intensity radiated field, emission to interfere with other susceptible equipments and crosstalk between cables or cable bundles, etc. For adequate design and placement of these cable and cable bundle networks, experiment is a usual way to reach various EMC

Received 26 October 2011, Accepted 2 December 2011, Scheduled 11 December 2011

* Corresponding author: Zhuo Li (lizhuo@nuaa.edu.cn).

requirements. Although we can accumulate much experience from the experiments, however, this cut and try procedure would be high cost and low efficiency. Accordingly, simulation can then in turn be a good alternative to save a lot of time and money at the very beginning of the design.

Immunity, emission and crosstalk issues of cables and cable bundles have always been the hot spot [1–6] since the multiconductor transmission line network (MTLN) theory [1] was put forward. Various simulation tools both in time and frequency domain were implemented to solve the complete cable and cable bundle model with or without the reference plane, in which the finite difference time domain method(FDTD) [8–10], the method of moments(MoM) [11], the finite element method(FEM) [12, 13], and their acceleration methods [14] are the representative ones. Deterministic results are usually obtained for a single and simple complete cable or cable bundle model, while statistic analysis [15] can predict the reasonable worst-case and give more meaningful results for a series randomly distributed and complex cable or cable bundle models. All these methods are based on the complete cable and cable bundle model that the computation burden becomes progressively heavier as the cable number increases.

The equivalent cable bundle method (ECBM), which is based on the assumption that the common-mode response is more critical than the differential-mode response when considering external EM waves coupling to the cables, emissions from the cables, crosstalk between different cables, has been successfully applied in the model reduction of the EM immunity [16], emissions [7] and crosstalk [17] of complex cable bundles over a large frequency range. In the original ECBM, the termination loads of the cable bundle are limited to frequency independent loads only, namely the pure resistance R, so the grouping result is frequency independent and can be applied in arbitrary excitation signal case. Although the ECBM [18] is very well suited for the cable bundle simplification not only in the MTLN but also in the MoM and cuts down a lot of computation complexity and time, it can not deal with arbitrary termination loads, frequency dependent loads in particular, which greatly narrows the applications of the ECBM. One tough problem is the cable grouping based on the comparison of both termination load impedances of each cable with the common-mode characteristic impedance of the whole model. The grouping result is obviously frequency dependent if cables are terminated in frequency dependent loads. Thus the original ECBM must be generalized to consider arbitrary loads in practical circumstances.

In this paper, a GECBM is proposed for the prediction of EM immunity, emissions and crosstalk issues of cable bundle terminated

in arbitrary loads. The whole paper is organized as follows. Section 2 presents the GECBM for cable EMC issues specifically. In Section 3, simulation results are given on the EM immunity, emissions and crosstalk problems to validate the proposed method, and finally, Section 4 draws some concluding remarks.

2. PRESENTATION OF THE GECBM FOR EMC ISSUES OF COMPLEX CABLE BUNDLE

Suffering from the limitation of frequency independent termination loads, the original ECBM can only be applied in a wide band excitation signal with frequency independent loads case or a single frequency signal with frequency dependent loads case. More often than not, however, the excitation signal is wide band and the termination loads are all frequency dependent.

In this section, a generalized ECBM is presented to consider arbitrary termination loads, including resistance R, inductance L, capacitance C and their arbitrary hybrid connections at near and far ends of cables shown in Fig. 1. The near and far end load impedances of Cable i are denoted by $\dot{Z}_{Ni}(f)$ and $\dot{Z}_{Fi}(f)$ $(i = 1, \ldots, n)$ respectively, which are complex values and frequency dependent. The GECBM is also based on the assumption that, as far as the EM coupling to the cable, EM emission from the cable and EM crosstalk between cables are concerned, the common-mode response is more critical than the differential-mode response. The fundamental point and superiority of the GECBM over the original ECBM is to get rid of the frequency restrictions by implementing a tradeoff between different grouping results at different frequencies for all termination loads at the grouping step. A definite grouping result over the whole frequency range of the

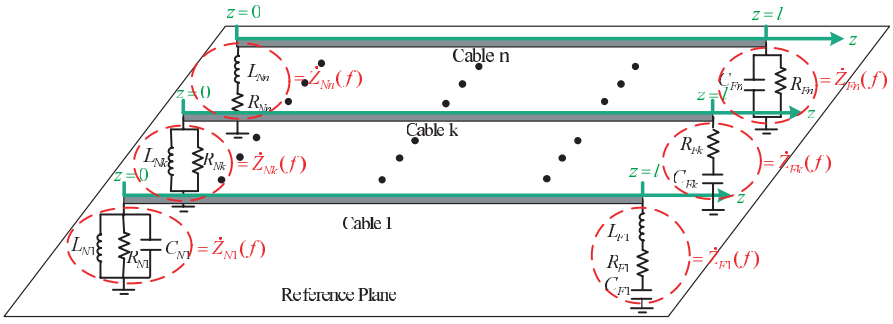

Figure 1. A cable bundle model with cables terminated in arbitrary loads at near and far ends.

excitation signal should be obtained by development of a new and adequate grouping criterion. On the whole, the complete GECBM can be implemented in five steps listed below:

2.1. Grouping of Conductors

For cable grouping in the GECBM, proper description and measurement by a definite value for the termination load impedance of each cable in the whole frequency range is a crucial step. One can easily think of the arithmetical average value (AAV) of the termination load impedance as a reference for comparison with the common mode characteristic impedance. It is feasible in cases when the impedance varies smoothly with frequency. However, for drastic variation impedance, the load is in series resonance or parallel resonance within a very narrow band, etc., the AAV may not accurately represent the overall impedance level within the frequency range we care.

Considering that in the frequency domain, the excitation signal and termination load impedance's different frequency components both contribute to the final response, we can apply the weighted average method (WAM) for the calculation of the weighted average value (WAV) of all the termination load impedances and the common mode characteristic impedance as comparative quantities. If the single sideband amplitude spectrum of the excitation signal $|\dot{V}_e(f)|$ can be depicted by Fig. 2(a), in which $f_{\max}$ denotes the upper cutoff frequency of the excitation signal. We remark that $f_{\max}$ must be properly chosen so that the energy distributed in $[0,\ f_{\max}]$ dominates more than 90 percent of the signal's total energy. Then the amplitude spectrum of the termination (near or far) load impedance $|\dot{Z}(f)|$ in $[0,\ f_{\max}]$ can be calculated and shown in Fig. 2(b). Thus, the cable grouping can be implemented in three steps:

Step I: Calculation of the WAV of all termination load impedances

As stated above, the WAV of near (far) end load impedance of the jth cable can be denoted by

$$\tilde{Z}_{N(F)j} = \frac{\sum\limits_{i=0}^{M}(\alpha_i|Z_{N(F)ji}|)}{\sum\limits_{i=0}^{M}\alpha_i}, \tag{1}$$

in which $Z_{N(F)ji}$ and α_i denote the near (far) end load impedance of the jth cable and the amplitude of the excitation signal at sampling frequency f_i $(i = 0, \ldots, M;\ j = 1, \ldots, n)$. M is the total frequency

sampling number in $[0, f_{\max}]$ and n is the total cable number in the complete cable bundle.

Step II: Calculation of the common mode characteristic impedance of the complete cable bundle model

Now we consider all the cables are lossy and the per-unit-length (p.u.l.)distributed resistance, conductance, inductance and capacitance matrices of the cable bundle can be denoted by $\mathbf{R}_{n\times n}$, $\mathbf{G}_{n\times n}$, $\mathbf{L}_{n\times n}$ and $\mathbf{C}_{n\times n}$ respectively. If we denote $\|\mathbf{A}\|$ as the sum of all the elements in matrix $\mathbf{A}_{n\times n}$, then $\|\mathbf{A}\| = \sum_{i=1}^{n}\sum_{j=1}^{n} a_{ij}$, in which a_{ij} is the ith row and jth column element of matrix $\mathbf{A}_{n\times n}$. According to the modal analysis [18], the common-mode impedance $\dot{Z}_{mc}$ of the lossy cable bundle model corresponds to the characteristic impedance of the common mode and can be written as

$$\dot{Z}_{mc} = \frac{1}{n}\sqrt{\frac{\|\dot{\mathbf{Z}}\|}{\|\dot{\mathbf{Y}}\|}} = \frac{1}{n}\sqrt{\frac{\|\mathbf{R}+j\omega\mathbf{L}\|}{\|\mathbf{G}+j\omega\mathbf{C}\|}} = \frac{1}{n}\sqrt{\frac{\sum_{i=1}^{n}\sum_{j=1}^{n}(R_{ij}+j\omega L_{ij})}{\sum_{i=1}^{n}\sum_{j=1}^{n}(G_{ij}+j\omega C_{ij})}}, \quad (2)$$

which is actually a complex value and frequency dependent. Thus, the WAV of the common mode characteristic impedance can be denoted by

$$\tilde{Z}_{mc} = \frac{\sum_{i=0}^{M}\left(\alpha_i|\dot{Z}_{mci}|\right)}{\sum_{i=0}^{M}\alpha_i}, \quad (3)$$

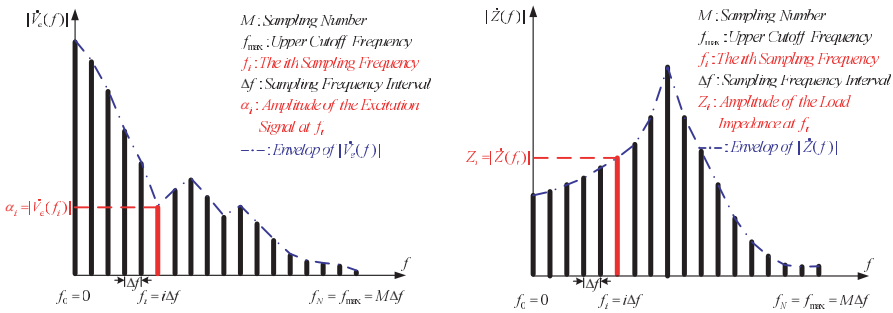

Figure 2. Amplitude spectrum of (a) excitation signal, (b) termination load impedance.

Table 1. Grouping criterion for the GECBM.

	Near End	Far End
Group 1	$\tilde{Z}_N > \tilde{Z}_{mc}$	$\tilde{Z}_F > \tilde{Z}_{mc}$
Group 2	$\tilde{Z}_N > \tilde{Z}_{mc}$	$\tilde{Z}_F < \tilde{Z}_{mc}$
Group 3	$\tilde{Z}_N < \tilde{Z}_{mc}$	$\tilde{Z}_F > \tilde{Z}_{mc}$
Group 4	$\tilde{Z}_N < \tilde{Z}_{mc}$	$\tilde{Z}_F < \tilde{Z}_{mc}$

in which $\dot{Z}_{mci}$ denotes the common mode characteristic impedance at sampling frequency f_i ($i = 0, \ldots, M$).

If the leakage current in the air and cable insulation layer is small enough and the resistance of each conductor can be omitted, the cables can be considered as lossless that $\|\mathbf{R}\| \approx 0$ and $\|\mathbf{G}\| \approx 0$. Thus the common-mode impedance of the lossless cable bundle model can be rewritten as

$$\tilde{Z}_{mc} = \frac{\sum\limits_{i=0}^{M} \alpha_i \left(|\dot{Z}_{mc}|\right)}{\sum\limits_{i=0}^{M} \alpha_i} = \frac{1}{n}\sqrt{\frac{\|\mathbf{L}\|}{\|\mathbf{C}\|}} = \frac{1}{n}\sqrt{\frac{\sum\limits_{i=1}^{n}\sum\limits_{j=1}^{n} L_{ij}}{\sum\limits_{i=1}^{n}\sum\limits_{j=1}^{n} C_{ij}}}, \tag{4}$$

which is real and frequency independent.

Step III: Cable grouping according to a new criterion

According to Table 1, four groups can be finally obtained by comparison of $\tilde{Z}_{N\,(F)}$ and $\tilde{Z}_{mc}$. The new criterion can be adopted for comprehensive consideration of both the end load impedance and the excitation signal's amplitude spectrums. We remark that the frequency sampling number M must be large enough to guarantee the grouping result stable. If $\tilde{Z}_{N(F)} \simeq \tilde{Z}_{mc}$, then this cable can be distributed in arbitrary group. This criterion can be naturally degenerated into the pure resistance case if $|Z_{N(F)j}|$ is constant and can be applied for both narrow and broad band excitation signal. In addition, it relieves the dependency of the grouping rule only on the termination load impedance value when the impedance is extremely high (or low) within very narrow band and extremely low (or high) outside this band, namely the parallel or series resonance. Examples of grouping cables terminated in parallel and series resonance loads are given in Section 3 to demonstrate the validity of the WAM. Indicated in previous works [7, 16, 17], all the conductors in the cable bundle participate in the grouping for EM immunity and emission problems

and for electromagnetic crosstalk problems the culprit and victim cables do not participate in the grouping.

2.2. Reduced Cable Bundle Matrices

Once the grouping process is completed, the computation of the reduced cable bundle matrices should follow those in [16] and is omitted here.

2.3. Reduced Cable Bundle Cross-section Geometry

The computation of the reduced cable bundle cross-section geometry is established through six optimization phases depicted in [16] and is also omitted here.

2.4. Reduced Cable Bundle Equivalent Termination Loads

The equivalent termination loads at each equivalent conductor ends can be categorized into three types:

a) Common-mode loads that connect conductor ends to the ground reference;
b) Differential loads that connect together two conductors belonging to the same group;
c) Differential loads that connect together two conductors belonging to different groups. This equivalence can be found in [16] and is omitted here.

2.5. Application of Different Numerical Methods to EMC Issues of the Reduced Cable Bundle Model

Once the reduced cable bundle model is obtained, we can apply the MTLN and MoM in the prediction of EM immunity, emission and crosstalk problems.

3. VALIDATIONS OF THE GECBM FOR EMC ISSUES THROUGH NUMERICAL SIMULATIONS

In this section, EMC issues including crosstalk, emission and immunity of a single complete cable bundle model are properly simplified through the GECBM. All the cables in the cable bundle are considered to be lossless single wire cable and the infinite ground plane is assumed to be perfect conducting in the simulations. Thus the WAV of the common

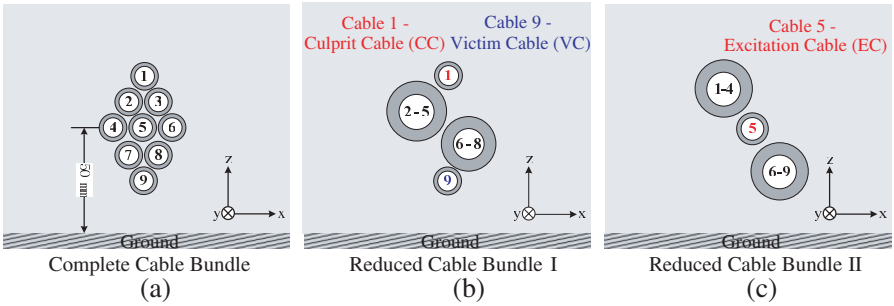

Figure 3. Cable bundle models (a) complete 9-conductor cable bundle model. (b) Reduced cable bundle model I for EM crosstalk problem. (c) Reduced cable bundle model II for EM emission and immunity problems.

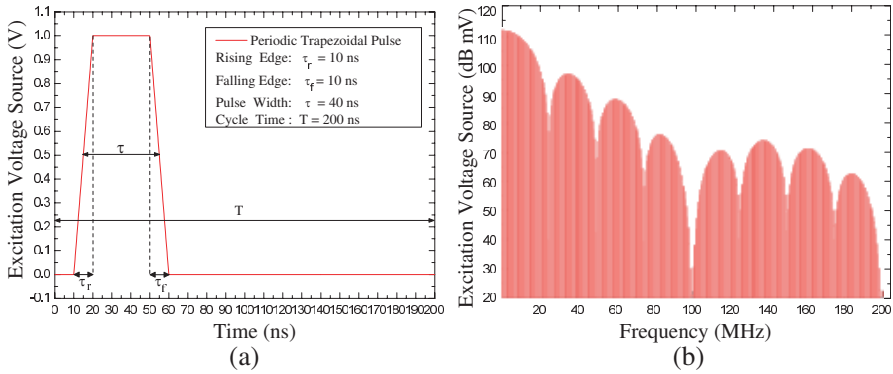

Figure 4. Case A: wave form of the excitation signal (a) time domain. (b) Frequency domain.

mode characteristic impedance reduced to (4). The 9-conductor point-to-point connected cable bundle, 1 m long, set above the infinite ground plane shown in Fig. 3(a) is investigated, in which each cable is a single wire conductor with a radius of 0.5 mm and is surrounded by dielectric coating with the thickness of 0.3 mm and the dielectric constant of $\epsilon_r = 2.5$ and $\mu_r = 1.0$. The cross section (x, z) coordinate of the center of each conductor are listed in Table 2.

Case A. EM crosstalk in a cable bundle

In this numerical simulation, the near end of Cable 1 (culprit cable) is excited with a voltage source of periodic trapezoidal pulse whose waveform is depicted in Fig. 4(a) and Cable 9 serves as the victim cable. The spectrum of the excitation signal in the frequency range $0 \sim 200$ MHz can be easily obtained through discrete Fourier transform and shown in Fig. 4(b). In order to demonstrate the applicability

Table 2. Case A: center coordinate (Unit: mm) and termination loads of the 9-conductor cable bundle ('+': in series; '||': in parallel; '$Z_{N\,(F)}$': near (far) end load; '$\tilde{Z}_{N\,(F)}$': weighted average impedance at near (far) end).

Conductor	1	2	3
$(x,\ z)$	(1.6, 2.8)	(0.8, 1.4)	(2.4, 1.4)
Z_N	$50\,\Omega$	$100\,\Omega + 0.1\,\mu\text{H}$	$100\,\Omega + 0.1\,\mu\text{H}$
$\tilde{Z}_N$		$101\,\Omega$	$101\,\Omega$
Z_F	$50\,\Omega$	$10\,\text{k}\Omega \parallel 10\,\text{pF}$	$10\,\text{k}\Omega + 0.1\,\mu\text{H}$
$\tilde{Z}_F$		$2537\,\Omega$	$10\,\text{k}\Omega$

Conductor	4	5	6
$(x,\ z)$	(0, 0)	(1.6, 0)	(3.2, 0)
Z_N	$50\,\Omega + 0.1\,\mu\text{H}$	$100\,\Omega \parallel 10\,\text{pF}$	$10\,\text{k}\Omega \parallel 500\,\text{nH} \parallel 31.66\,\text{pF}$ $0.1\,\Omega + 80\,\text{nH} + 351.8\,\text{pF}$
$\tilde{Z}_N$	$52\,\Omega$	$99\,\Omega$	$195\,\Omega$ $824\,\Omega$
Z_F	$5\,\text{k}\Omega \parallel 10\,\text{pF}$	$100\,\text{k}\Omega \parallel 100\,\text{pF}$	$100\,\Omega + 0.1\ \mu\text{H}$
$\tilde{Z}_F$	$1932\,\Omega$	$1495\,\Omega$	$101\,\Omega$

Conductor	7	8	9
$(x,\ z)$	(0.8, −1.4)	(2.4, −1.4)	(1.6, −2.8)
Z_N	$15\,\text{k}\Omega \parallel 400\,\text{nH} \parallel 17.59\,\text{pF}$ $0.1\,\Omega + 40\,\text{nH} + 253.3\,\text{pF}$	$20\,\text{k}\Omega \parallel 400\,\text{nH} \parallel 9.895\,\text{pF}$ $0.2\,\Omega + 20\,\text{nH} + 258.5\,\text{pF}$	$50\,\Omega \parallel 200\,\text{pF}$
$\tilde{Z}_N$	$162\,\Omega$ $870\,\Omega$	$98\,\Omega$ $867\,\Omega$	
Z_F	$100\,\Omega \parallel 10\,\text{pF}$	$50\,\Omega + 0.1\,\mu\text{H}$	$50\,\Omega \parallel 200\,\text{pF}$
$\tilde{Z}_F$	$99\,\Omega$	$52\,\Omega$	

of the weighted average criterion, two extreme examples when the end load impedance varies sharply within a narrow band, namely the parallel and series resonance loads are taken into consideration. The termination loads of all the cables of this cable bundle in both examples are listed in Table 2. In Example I parallel resonance happens at

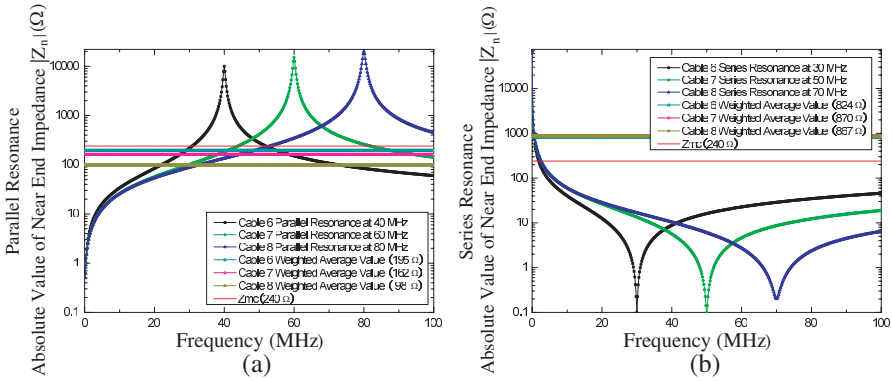

Figure 5. Case A: Absolute values of the near end impedances on Cables 6 $\sim$ 8 and the comparison of their weighted average values with the common mode characteristic impedance $\tilde{Z}_{mc}$. (a) Parallel resonance. (b) Series resonance.

40 MHz, 60 MHz and 80 MHz at near end of Cables 6 $\sim$ 8 respectively and in Example 2 series resonance happens at 30 MHz, 50 MHz and 70 MHz at near end of Cables 6 $\sim$ 8 respectively shown in Fig. 5(a), (b). The p.u.l.inductance $[L]$ (in nanohenry/meter) and capacitance $[C]$ matrices (in picoferad/meter) of Cables 2 $\sim$ 8 in the cable bundle are listed in (5) and (6).

$$[L] = \begin{bmatrix} 1015 & 809 & 806 & 801 & 736 & 732 & 714 \\ & 1015 & 736 & 801 & 806 & 714 & 732 \\ & & 1011 & 801 & 716 & 802 & 732 \\ & & & 988 & 800 & 797 & 797 \\ & & & & 1011 & 732 & 802 \\ & & & & & 1007 & 801 \\ & & & & & & 1007 \end{bmatrix}_{7\times7}, \tag{5}$$

$$[C] = \begin{bmatrix} 43.8 & -15.0 & -14.7 & -9.7 & -0.8 & -0.8 & -0.4 \\ & 43.8 & -0.8 & -9.7 & -14.7 & -0.4 & -0.8 \\ & & 43.9 & -10.0 & -0.4 & -14.7 & -0.8 \\ & & & 59.0 & -10.0 & -9.7 & -9.7 \\ & & & & 43.9 & -0.8 & -14.7 \\ & & & & & 43.9 & -15.0 \\ & & & & & & 43.9 \end{bmatrix}_{7\times7}. \tag{6}$$

According to the grouping process in Section 2, the upper cutoff frequency $f_{\max}$ can be chosen as $f_{\max} = 1/\tau_r = 100$ MHz and the amplitude spectrum of the excitation signal and the termination load impedance are sampled with the sampling interval $\Delta f = 0.2$ MHz

in the frequency range $0 \sim 100\,\text{MHz}$. The amplitude α_i of the excitation signal at sampling frequency f_i ($i = 0, \ldots, 500$) can be easily obtained from Fig. 4(b). Thus, the weighted average common mode characteristic impedance $\tilde{Z}_{mc}$ can be calculated by Eqs. (4) $\sim$ (6) and equals $240\,\Omega$. The weighted average values $\tilde{Z}_{N(F)}$ of the near and far ends of Cables 2 $\sim$ 8 can be calculated by Eq. (1) and are listed in Table 2. According to the grouping criterion, for both parallel and series resonance cases, the 7 conductors can be sorted into two groups: Group 1 (Cables 2 $\sim$ 5) and Group 2 (Cables 6 $\sim$ 8) shown in Fig. 3(b).

After some simple calculations, the p.u.l.parameter matrices $[L]$ (in nanohenry/meter) and capacitance $[C]$ (in picoferad/meter) of the reduced cable bundle model can be written as follows

$$[L_{\text{reduced}}] = \begin{bmatrix} 846 & 757 \\ & 855 \end{bmatrix}_{2\times 2}, \tag{7}$$

$$[C_{\text{reduced}}] = \begin{bmatrix} 129.3 & -122.1 \\ & 129.5 \end{bmatrix}_{2\times 2}. \tag{8}$$

After applying the six-phase procedure described in [16], we obtain the cross-section geometry of the reduced cable bundle model composed of four equivalent conductors shown in Fig. 3(b). And the equivalent termination loads connected to each end of all conductors in the reduced cable bundle can be easily obtained using Step 4 in Section 2. Also, the related center coordinate, radius, and insulator thickness are listed in Table 3. The near and far ends crosstalk voltage on Cable 9 can finally be obtained by applying the MTLN to the complete and reduced models shown in Figs. 6 and 7. It is obvious

Table 3. Some parameters of the reduced cable bundles (Unit: mm).

Reduced Model in Fig. 3(c)			
Conductor	1–4	5	6–9
(x, z)	$(-0.4, 1.4)$	$(1.6, 0.0)$	$(3.6, -1.4)$
Conductor Radius	1.6	0.75	1.6
Insulator Thickness	0.3	0.1	0.3
Reduced Model in Fig. 3(b)			
1	2–5	6–8	9
$(1.6, 2.8)$	$(0.3, 0.7)$	$(3.0, -0.9)$	$(1.6, -2.8)$
0.5	1.5	1.4	0.5
0.3	0.1	0.1	0.3

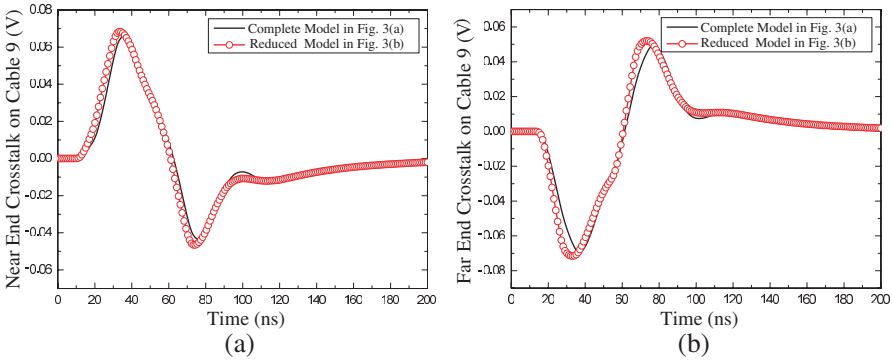

Figure 6. Case A: comparison of the crosstalk voltage in the time domain on Cable 9 between the complete and reduced cable bundle models when parallel resonance happens at the near end of Cables 6 $\sim$ 8. (a) Near end. (b) Far end.

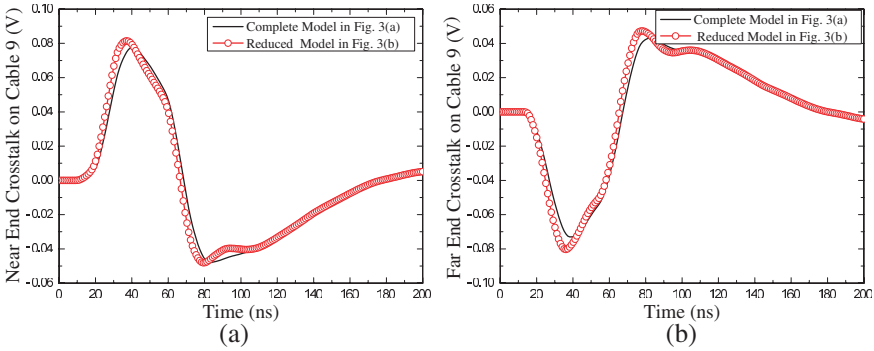

Figure 7. Case A: comparison of the crosstalk voltage in the time domain on Cable 9 between the complete and reduced cable bundle models when series resonance happens at the near end of Cables 6 $\sim$ 8. (a) Near end. (b) Far end.

that the reduced model shows good agreement with the complete one by using the GECBM in both resonance cases.

Case B. EM emissions of a cable bundle

The second numerical validation concerns the radiation pattern and near electric field of the cable bundle shown in Fig. 3(a). In this case, the termination loads of the 9 conductors are listed in Table 4 and Cable 5 is excited at its near end by a periodic trapezoidal pulse voltage source of 1 V magnitude with rising and falling edge $\tau_r = \tau_f = 0.3$ ns, pulse width $\tau = 1$ ns and cycle time $T = 3$ ns. Thus the upper cutoff frequency $f_{\max} = 1/\tau_r = 3.3$ GHz and the complete cable bundle can be simplified to a reduced one shown in Fig. 3(c) through the above

Table 4. Case B & C: termination loads of the 9-conductor cable bundle.

Conductor	1	2	3	4
Z_N	$50\,\Omega$	$150\,\Omega$	$100\,\Omega + 5\,\text{nH}$	$50\,\Omega + 5\,\text{nH}$
$\tilde{Z}_N$	$50\,\Omega$	$150\,\Omega$	$100\,\Omega$	$50\,\Omega$
Z_F	$50\,\Omega$	$100\,\Omega + 4.7\,\text{nH}$	$100\,\Omega \parallel 2\,\text{pF}$	$100\,\Omega$
$\tilde{Z}_F$	$50\,\Omega$	$100\,\Omega$	$99\,\Omega$	$100\,\Omega$

5	6	7	8	9
$5\,\text{k}\Omega$	$1\,\Omega$+200 nH +20 pF	$200\,\text{k}\Omega$	$6\,\text{k}\Omega + 10\,\mu\text{H}$	$10\,\Omega + 200\,\text{nH}$ + 20 pF
$5\,\text{k}\Omega$	$1589\,\Omega$	$200\,\text{k}\Omega$	$6562\,\Omega$	$1590\,\Omega$
$150\,\Omega \parallel 1\,\text{nF}$	$5\,\text{k}\Omega$	$10\,\text{k}\Omega \parallel 20\,\text{nH}$ $\parallel 2\,\text{nF}$	$20\,\text{k}\Omega$	$15\,\text{k}\Omega \parallel 2\,\text{nH}$ $\parallel 2\,\text{nF}$
$29\,\Omega$	$5\,\text{k}\Omega$	$272\,\Omega$	$20\,\text{k}\Omega$	$385\,\Omega$

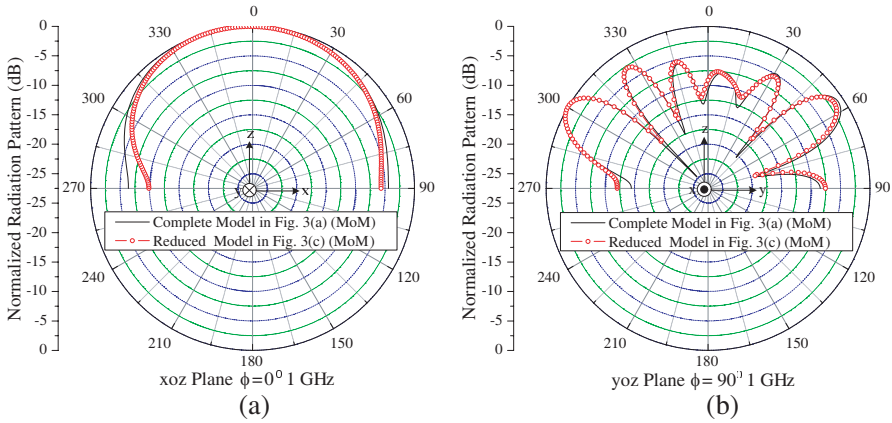

Figure 8. Case B: MoM computations of the normalized radiation pattern of the complete and the reduced cable bundle models at 1 GHz. (a) *xoz* plane $\phi = 0°$. (b) *yoz* plane $\phi = 90°$.

equivalence procedure. The p.u.l. inductance $[L]$ and capacitance $[C]$ matrices as well as all the parameters of cables in the complete and reduced cable bundle models are not listed here for simplicity. The weighted average common-mode characteristic impedance $\tilde{Z}_{mc}$ of the 9-conductor cable bundle equals $224\,\Omega$. According to the grouping criterion, the 9 conductors can be sorted into three groups: Group 1 (Cables $1 \sim 4$), Group 2 (Cable 5) and Group 3 (Cables $6 \sim 9$) and the cross-section geometry of the reduced cable bundle composed of three equivalent conductors are shown in Fig. 3(c). The reduced cable

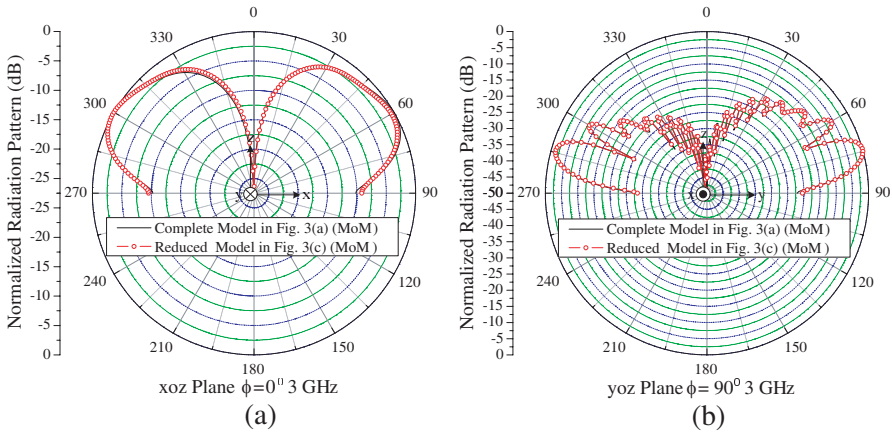

Figure 9. Case B: MoM computations of the normalized radiation pattern of the complete and the reduced cable bundle models at 3 GHz. (a) xoz plane $\phi = 0°$. (b) yoz plane $\phi = 90°$.

bundle model is then introduced in the three dimensional (3D) full wave simulation code for the calculation of the EM emission of the cable bundle both at 1 GHz and 3 GHz. We have calculated the normalized radiation pattern in the $\phi = 0°$ and $\phi = 90°$ planes according to the coordinate in Fig. 3. Figs. 8 and 9 present the results obtained at 1 GHz and 3 GHz for both cable bundle models respectively. The near electric field is also calculated for both cable bundle models at an observation point of $x = 3$ cm, $y = 60$ cm, $z = 3$ cm coordinates shown in Fig. 10(a). This observation point is located at a distance of 3.6 cm from the closet point of the cable bundle. The very good agreement of all the radiation patterns and near-electric field for both cable bundle models entirely validate the method for EMC emission problems.

Case C. EM immunity of a cable bundle

Considering the cable bundle in Fig. 3(a) illuminated by a plane wave with a 5 V/m magnitude toward $+y$ direction and an electric field along z direction, common mode current extraction can be reproduced on the reduced cable bundle model shown in Fig. 3(c) by the GECBM. The common mode current is calculated in Group 1 by averaging the sum of all the currents at one end of Cables $1 \sim 4$ for both cable bundle models. Fig. 10(b) presents the comparison result and good agreement in the frequency range $0 \sim 500$ MHz shows that the reduced cable bundle model can be introduced in the 3D full wave simulation tools to reproduce the cable bundle common mode current.

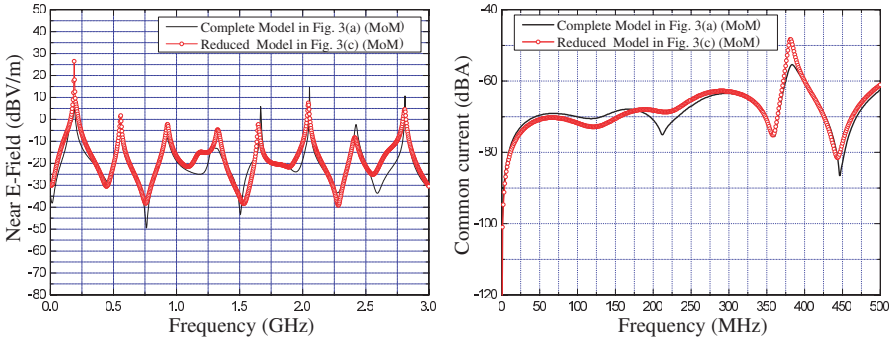

Figure 10. (a) Case B: MoM computations of the near-radiated electric field for the complete and the reduced cable bundle models. (b) Case C: MoM computations of the common-mode current induced at one end of the complete and the reduced cable bundle models.

Table 5. Computation time and memory comparison between the complete and reduced cable bundle models (Case B: 3 GHz; Case C: 0 to 500 MHz, 20 frequency sampling points).

Case	Complete Model	Reduced Model	Ratio
B&C:Number of total unknowns	1569	789	1.99
B&C:Number of unknowns due to triangles	444	378	1.17
B&C:Number of unknowns due to segments	1125	411	2.74
B: Calculation of matrix elements(s)	156.094	55.782	2.8
B: Calculation of far field(s)	41.656	38.016	1.1
B: Calculation of near E-field(s)	2.313	0.953	2.43
B: Required memory (MByte)	25.511	7.902	3.23
B: Total calculation time(s)	202.641	95.828	2.11
C: Calculation of matrix elements(s)	117.016	56.797	2.06
C: Required memory (MByte)	25.511	8.157	3.13
C: Total calculation time(s)	2541	695	3.66

4. CONCLUSIONS

In this work, the GECBM is presented in detail for the analysis of the EM issues of complex cable bundle. EM crosstalk, emission and immunity examples all exhibit the validity and ability of this method both with MTLN at "low frequencies" and MoM at "high frequencies"

in the simulation of the response of cable bundle terminated in arbitrary loads, which is quite different from previous works. The authors are confident that the GECBM can find potential applications in the analysis and design of more realistic and complex cable bundles.

The total computation time is reduced by a factor of 3 after equivalence of the complete model for Case A by using the MTLN. In Table 5, the computation times and memory required for the MoM modeling of both cable bundles at the frequency of 3 GHz for Case B and from 0 to 500 MHz for Case C are presented. The computations have been performed on a 3 GHz processor and a 2 GB RAM memory computer. All these results fully demonstrate that the GECBM can significantly reduce the prediction time and memory requirement. It could be expected that with the cable number in the original complete cable bundle increases, we can cut down much more computation time and memory.

Some limitations of this work are listed below and discussed.

1) The pure computation time of the reduced model using the MTLN and the MoM has been reduced significantly. However, the extra equivalence procedure and optimization time should also be considered and must be further accelerated to fulfill the requirements of realistic applications in a quick automatic manner.
2) The excitation signal is added to only one cable.When multiple signals are excited, we can follow the theory in [4] to consider more realistic cases.

In the near future, we will concentrate on the EM crosstalk, emission and immunity prediction of cable bundles in realistic vehicles through the combination of the full-wave simulation method and the GECBM.

ACKNOWLEDGMENT

This work was supported in part by the National Natural Science Foundation of China for Young Scholars under Grant No: 61102033 and in part by the Foundation of State Key Laboratory of Millimeter Waves, Southeast University, P. R. China under Grant No. K201003.

REFERENCES

1. Paul, C. R., *Analysis of Multiconductor Transmission Lines*, Wiley-Interscience, New York, 1994.

2. Paul, C. R., "Frquency response of multiconductor transmission lines illuminated by an electromagnetic field," *IEEE Trans. on Electromagn. Compat.*, Vol. 18, No. 4, 183–190, Nov. 1976.
3. Kami, Y. and R. Sato, "Transient response of a transmission line excited by an electromagnetic pulse," *IEEE Trans. on Electromagn. Compat.*, Vol. 30, No. 4, 457–462, Nov. 1988.
4. Lin, D.-B., F.-N. Wu, W. S. Liu, C. K. Wang, and H.-Y. Shih, "Crosstalk and discontinuities reduction on multi-module memory bus by particle swarm optimization," *Progress In Electromagnetics Research*, Vol. 121, 53–74, 2011.
5. Xie, H., J. Wang, D. Sun, R. Fan, and Y. Liu, "Spice simulation and experimental study of transmission lines with TVSs excited by EMP," *Journal of Electromagnetic Waves and Applications*, Vol. 24, No. 2–3, 401–411, 2010.
6. Koo, S.-K., H.-S. Lee, and Y. B. Park, "Crosstalk reduction effect of asymmetric stub loaded lines," *Journal of Electromagnetic Waves and Applications*, Vol. 25, No. 8–9, 1156–1167, 2011.
7. Andrieu, G., A. Reineix, X. Bunlon, J. P. Parmantier, L. Koné, and B. Démoulin, "Extension of the "equivalent cable bundle method" for modeling electromagnetic emissions of complex cable bundles," *IEEE Trans. on Electromagn. Compat.*, Vol. 51, No. 1, 108–118, Feb. 2009.
8. Orlandi, A. and C. R. Paul, "FDTD analysis of lossy, multiconductor transmission lines terminated in arbitrary loads," *IEEE Trans. on Electromagn. Compat.*, Vol. 38, No. 3, 388–399, Aug. 1996.
9. Trakadas, P. T. and C. N. Capsalis, "Validation of a modified fdtd method on non-uniform transmission lines," *Progress In Electromagnetics Research*, Vol. 31, 311–329, 2001.
10. Wang, J., W.-Y. Yin, J.-P. Fang, and Q.-F. Liu, "Transient responses of coaxial cables in an electrically large cabin with slots and windows illuminated by an electromagnetic pulse," *Progress In Electromagnetics Research*, Vol. 106, 1–16, 2010.
11. Hsu, C.-I. G., R. F. Harrington, K. A. Michalski, and D. Zheng, "Analysis of multiconductor transmission lines of arbitrary cross section in multilayered uniaxial media," *IEEE Trans. on Microw. Theory and Tech.*, Vol. 41, No. 1, 70–78, Jan. 1993.
12. Pantic, Z. and R. Mittra, "Quasi-TEM analysis of microwave transmission lines by the finite-element method," *IEEE Trans. on Microw. Theory and Tech.*, Vol. 34, No. 11, 1096–1103, Nov. 1986.
13. Shamaileh, K. A. A., A. M. Qaroot, and N. I. Dib, "Non-uniform

transmission line transformers and their application in the design of compact multi-band Bagley power dividers with harmonics suppression," *Progress In Electromagnetics Research*, Vol. 113, 269–284, 2011.

14. Bagci, H., A. E. Yilmaz, Jian-Ming Jin, and E. Michielssen, "Fast and rigorous analysis of emc/emi phenomena on electrically large and complex cable-loaded structures," *IEEE Trans. on Electromagn. Compat.*, Vol. 49, No. 2, 361–381, May 2007.
15. Wu, M., D. G. Beetner, T. H. Hubing, H. X. Ke, and S. S. Sun, "Statistical prediction of "reasonable worst-case" crosstalk in cable bundles," *IEEE Trans. on Electromagn. Compat.*, Vol. 51, No. 3, 842–851, Aug. 2009.
16. Andrieu, G., L. Koné, F. Bocquet, B. Démoulin, and J. P. Parmantier, "Multiconductor reduction technique for modeling common-mode currents on cable bundles at high frequency for automotive applications," *IEEE Trans. on Electromagn. Compat.*, Vol. 50, No. 1, 175–184, Feb. 2008.
17. Li, Z., Z. J. Shao, J. Ding, Z. Y. Niu, and C. Q. Gu, "Extension of the "equivalent cable bundle method" for modeling crosstalk of complex cable bundles," *IEEE Trans. on Electromagn. Compat.*, Vol. 53, No. 4, 1040–1049, Nov. 2011.
18. Andrieu, G., X. Bunlon, L. Koné, J. P. Parmantier, B. Démoulin, and A. Reineix, "The 'equivalent cable bundle method': an efficient multiconductor reduction technique to model industrial cable networks," *New Trends and Developments in Automotive System Engineering*, InTech, Jan. 2011.